THE JOURNAL OF BIOLOGICAL CHEMISTRY
Vol. 271, No. 34, Issue of August 23, pp. 20470–20478, 1996

Printed in U.S.A.

Kinetics of Interaction of Rab5 and Rab7 with Nucleotides and Magnesium Ions*

(Received for publication, January 4, 1996, and in revised form, May 17, 1996)

Iris Simon‡, Marino Zerial§, and Roger S. Goody‡¶

From the ‡Abteilung Physikalische Biochemie, Max-Planck-Institut für Molekulare Physiologie, Rheinlanddamm 201, 44139 Dortmund and the §European Molecular Biology Laboratory, Meyerhofstrasse, 69012 Heidelberg, Federal Republic of Germany

We describe here the kinetics of the interaction of GTP and GDP with the small GTP-binding proteins Rab5 and Rab7. It was possible to make use of the intrinsic fluorescence of these proteins, since Rab5 contains two and Rab7 three tryptophan residues, respectively. With both enzymes, there is a significant decrease in fluorescence on binding GTP and an increase on binding GDP. As with the small GTP-binding protein Ha-Ras p21 and with EF-Tu, nucleotide binding occurs in at least two steps and is describable in terms of a relatively weak initial interaction followed by a highly irreversible isomerization of the protein-nucleotide complex, which results in a change in the fluorescence properties. Dissociation of GDP and GTP could be followed in a time-dependent manner using fluorescently labeled GDP (methylanthraniloyl GDP) as displacing agent and taking advantage of substantial fluorescent energy transfer from tryptophan to the nucleotide. Fluorescence techniques could also be used to quantitate the interaction of Mg^{2+} ions with the GTP and GDP forms of Rab7, and it was shown that the metal ion was bound ~1000-fold more strongly to the GTP than the GDP form. The rate of GTP cleavage by the two proteins differed by a factor of ~20 (2×10^{-3} s^{-1} for Rab5 and 9×10^{-4} s^{-1} for Rab7 at 37 °C). Both proteins showed significant discrimination against xanthosine 5′-*O*-diphosphate (K_d ~10^3-fold higher than that of GDP) and dramatic discrimination against ADP or ATP (K_d ~10^6-fold higher than that of GDP). The results demonstrate a high degree of mechanistic similarity between the Rab proteins and other GTP-binding proteins, which have been examined in detail, including Ha-Ras p21, Ran, and EF-Tu.

The Rab proteins are members of the Ras superfamily of small GTP-binding proteins. They are involved in protein trafficking in the cell and have been implicated in the mechanisms by which transport vesicles identify and fuse with their target compartment (1–4). Like the other members of the Ras superfamily, and in common with other classes of GTP-binding proteins, they cycle between the GTP- and GDP-bound forms and appear to share at least some of the general properties of the family, including interaction with nucleotide exchange factors (Refs. 5–8), in some cases (and perhaps in all) with GTPase-activating proteins (GAPs[1]; Refs. 9 and 10) and with effector molecules. A class of molecules which appear to be critical for the role of Rab proteins are GDP dissociation inhibitors, which bind Rabs that are prenylated (doubly geranylgeranylated near the C terminus) in a specific manner and deliver them to their respective membranes, as well as retrieving them from these locations (11). A related molecule, the Rab escort protein (REP), is necessary for prenylation of Rabs (catalyzed by a geranylgeranyltransferase) and is also involved in delivery to, and retrieval of Rabs from, membrane compartments (12). Other molecules that interact with Rab proteins have also been identified. These include rabphilin-3A, which is a putative target of Rab3A/3C in synaptic vesicles and appears to be involved in neurotransmitter release (13, 14). A protein named rabaptin-5 has been identified as an effector of Rab5. This protein interacts with Rab5 in a GTP-dependent manner and appears to be essential for early endosome fusion (15).

In comparison to the intensively investigated Ras protein, relatively little information is available at the molecular level on the structure of Rabs and their GTPase cycle. In the present paper we describe fluorescence methods for the detailed investigation of the interaction of nucleotides with Rab5 and Rab7 and discuss the results in relation to the recently determined three-dimensional structure of Rab7.[2] The results show a striking similarity between the Rab molecules and other members of the Ras superfamily. In particular, for both GTP and GDP, interaction with the nucleotide-free protein can be described as an initial weak, rapid binding followed by a quasi-irreversible isomerization of the protein-nucleotide complexes. Spontaneous dissociation of both GDP and GTP is extremely slow, suggesting very tight regulation of the activity of the Rab proteins. The quantitative results form the basis for understanding the mode of action of Rab molecules both at the mechanistic and cell biological levels.

MATERIALS AND METHODS

Expression Plasmids

DNA fragments containing the coding regions of Rab5 and Rab7 DNAs (16) were obtained by polymerase chain reaction amplification using the oligonucleotides AGTCGGATCCATATGGCTAATCGAGGAGCAACAAGA (Rab5) and AGTCGGATCCATATGACCTCTAGGAAGAAAGTGTTG (Rab7) in combination with the SP6 primer and pGEM-Rab5 and pGEM-Rab7 as the templates, respectively. In the case of Rab5, the amplified DNA fragments was cut with *Nde*I and *Bam*HI and inserted into the corresponding sites of the pET3a vector (17). The Rab7 DNA fragment was cut with *Kpn*I, the ends polished with T4 DNA

* The costs of publication of this article were defrayed in part by the payment of page charges. This article must therefore be hereby marked "*advertisement*" in accordance with 18 U.S.C. Section 1734 solely to indicate this fact.

¶ To whom correspondence should be addressed. Tel.: 49-231-1206-380; Fax: 49-231-1206-229; E-mail: goody@mpi-dortmund.mpg.de.

[1] The abbreviations used are: GAP, GTPase-activating protein; mant-GDP(GTP), methylanthraniloyl guanosine di(tri)phosphate; $GppCH_2p$, guanosine 5′-*O*-(β,γ-methylenetriphosphate); GppNHp, guanosine 5′-(β,γ-imido)triphosphate; GTPγS, guanosine 5′-*O*-(γ-thiotriphosphate); GDI, guanosine nucleotide dissociation inhibitor 7; XDP, xanthosine 5′-*O*-diphosphate.

[2] P. Metcalf, manuscript in preparation.

polymerase and restricted with *Nde*I, and inserted into the pET3a vector. To do this, the plasmid was cut with *Bam*HI and, after filling in the protruding ends with *Escherichia coli* Klenow fragment, with *Nde*I. Protein expression was in *E. coli* BL 21 (DE3) cells at 37 °C.

Proteins

Rab7—50 g of cells in which Rab7 expression had been induced with isopropyl-β-D-thiogalactopyranoside were suspended in would of a buffer containing 64 mM Tris·HCl (pH 8.5), 8 mM $MgCl_2$, 2 mM EDTA, 1 mM dithioerythritol, 10 μM NaN_3 and treated for 1 h at 4 °C with Lysozyme (200 mg), phenylmethylsulfonyl fluoride (2 mM), and EDTA (2 mM) were included as protease inhibitors. 4% Sodium-desoxycholate (7 ml) was then added, followed after 10 min by 20 mg of DNase I and 10 mM $MgCl_2$. After ~1 h, cell fragments were removed by centrifugation at 17,700 × *g* for 30 min at 4 °C, and the supernatant was applied to a column of Q-Sepharose (600 ml) equilibrated with the buffer described above for cell lysis. After washing with 1 column volume, the column was developed with a linear gradient from 0 to 200 NaCl (10 column volumes). Rab7 was eluted between 50 and 100 mM NaCl. Detection and identification were achieved by Western blotting and a GDP filter binding test (18). Pooled fractions containing Rab7 were dialyzed overnight at 4 °C against 50 mM sodium acetate buffer (pH 4), and precipitated protein material was removed by centrifugation. A second chromatographic procedure was performed on a column (300 ml) of S-Sepharose, which was developed with 10 column volumes of a linear gradient of 0–600 NaCl in sodium acetate buffer. After identification and pooling of fractions containing Rab7, they were dialyzed overnight against a buffer that was identical to the buffer used for cell lysis except that the pH was adjusted with HCl to 7.6. Ammonium sulfate was added to a concentration of 2.4 M, and precipitated protein was collected by centrifugation. The pellet was dissolved in the buffer used for the last dialysis and applied to a Superdex 75 column (330 ml). After elution with the same buffer and identification of Rab7, the protein solution was concentrated (Amicon or Zentriprep) to ~10 mg/ml. The yield of homogeneous protein (SDS-electrophoresis) was ~50 mg.

Rab5—Purification of Rab5 was as described (19) except that the protein was further purified by gel filtration as described above for Rab7.

Nucleotides

Methylanthraniloyl derivatives of GDP and GTP were prepared as described (20). Nucleotides were separated analytically by HPLC as described previously (18, 20).

Nucleotide Exchange

The tightly bound GDP present in purified samples of Rab7 and Rab5 could be exchanged against other nucleotides (GTP, GppNHp, mant-GTP/GDP) in the presence of EDTA, followed by gel filtration to remove excess nucleotide.

Preparation of Nucleotide-free Rab5 and Rab7

Removal of tightly bound GDP without replacement by another nucleotide was performed essentially as described previously for Ha-ras p21 (20). Since the rate of GDP release from the Rab proteins is even slower than for Ras, more care had to be taken to ensure removal of excess Mg^{2+}, which slows down the rate of nucleotide dissociation. This was achieved by incubation of the protein with 10 mM EDTA prior to passage over a Sephadex PD-10 G-25 column to remove excess EDTA, since this would otherwise inhibit the enzymes used for removal of GDP. After addition of a 10-fold excess of $GppCH_2p$ over protein to this solution, it was brought to 200 mM with respect to ammonium sulfate, and 5 units/mg of phosphodiesterase-free alkaline phosphatase were added. Disappearance of GDP was monitored by HPLC, and typically 24 h at 18 °C, were needed for complete degradation to guanosine. Phosphodiesterase (5 units/mg) was then added, and the incubation continued at 15 °C until the $GppCH_2p$ was also degraded to guanosine. The resulting solution could be shock-frozen and stored at −80 °C. Before use, precipitated guanosine was removed by centrifugation, and if neccessary, remaining guanosine was removed by gel filtration.

Fluorescence Measurements

Fluorescence spectra and long time fluorescence measurements (GTPase or nucleotide dissociation reactions) were performed with an SLM 8000 spectrophotometer (Aminco, Silver Spring, MD). Rapid kinetics were measured with a stopped flow apparatus (High Tech Scientific, Salisbury, United Kingdom) with protein concentrations of 0.5–1.0 μM. Excitation of tryptophan fluorescence was at 290 nm, with detection through a 320 nm cut-off filter. Fluorescence of mantGDP was excited either directly at 370 nm or via FRET at 290 nm, with emission through a 389 nm cut-off filter. Data collection and primary analysis for determination of rate constants were performed with the package from High Tech Scientific, while secondary analysis was with the program Grafit 3.0 (Erithacus software).

GTPase Measurements

GTP hydrolysis was assayed as a function of time by HPLC on a C_{18} reversed phase column in the presence of tetrabutylammonium bromide under isocratic conditions (18). After performing an exchange reaction (GTP against GDP) as described above, the GTPase reaction was started by addition of 10 mM Mg^{2+} at 37 °C, and aliquots were analyzed at appropriate time intervals. To examine the dissociation kinetics of GTP simultaneously with (*i.e.* in competition with) GTP hydrolysis, a 40–50-fold excess of GDP was added a few seconds after starting the reaction with $MgCl_2$.

Fluorescence measurements of GTPase activity were performed in a fluorescence spectrophotometer, with excitation at 290 nm, detecting emission at 340 nm in 40 mM Hepes buffer at pH 7.5. The reaction was started by addition of 10 mM $MgCl_2$ at 37 °C.

RESULTS

Preparation of Nucleotide-free Proteins—A prerequisite for a detailed transient kinetic investigation of the interaction of an enzyme with its substrate is the availability of relatively large amounts of protein without a bound ligand at its active site. While bacterial expression systems have been developed over the past few years for a number of small GTP-binding proteins, the proteins are isolated invariably with a stoichiometric amount of strongly bound GDP at the active site, which makes detailed investigations of nucleotide binding and hydrolysis, or even the measurement of the affinity to GDP, difficult (21). A method that was originally developed to prepare nucleotide-free Ha-Ras p21 was used to prepare nucleotide-free Rab5 and Rab7 (20). The basic principle of this method is that GDP is replaced by the less strongly bound GTP analog, $GppCH_2p$, while GDP is degraded by alkaline phosphatase. In a second step, the GTP analog is degraded to GMP by phosphodiesterase, the GMP being then further degraded by alkaline phosphatase to guanosine. The low affinity of guanosine (20) means that the protein preparation can be regarded as ligand-free, even without separation from guanosine.

Application of the procedure outlined here to Rab5 and Rab7 was successful, but only if particular care was taken to reduce the free Mg^{2+} concentration as far as possible. The much slower rate of GDP release of the Rab proteins compared with Ras (see below) leads to longer incubation times for both steps of the preparation, and this can lead to difficulties because of the limited stability of the nucleotide-free proteins. To shorten the incubation times, advantage is taken of the known Mg^{2+} dependence of the rate of nucleotide release from complexes with the small GTP-binding proteins (22). Since divalent metal chelaters cannot be used because of their inhibition of alkaline phosphatase, the free magnesium concentration is reduced as far as possible by gel filtration in a Mg^{2+}-free buffer (see "Materials and Methods"). Rigorous application of this procedure, together with careful control of temperature during the procedure, led to the production of high yields of nucleotide-free Rab5 and Rab7, and these could be used for investigations of the association reactions of the proteins with GTP and GDP.

Most of the detailed work reported here is for the protein Rab7, which was available in larger quantities than Rab5. However, a number of key experiments were also performed with the latter protein and are described here.

Intrinsic Fluorescence—In contrast to Ha-Ras p21, both Rab proteins have tryptophan residues (positions 75 and 114 in Rab5; positions 62, 102, and 142 in Rab7; the first two are in structurally equivalent positions). These are situated 15, 8.4,

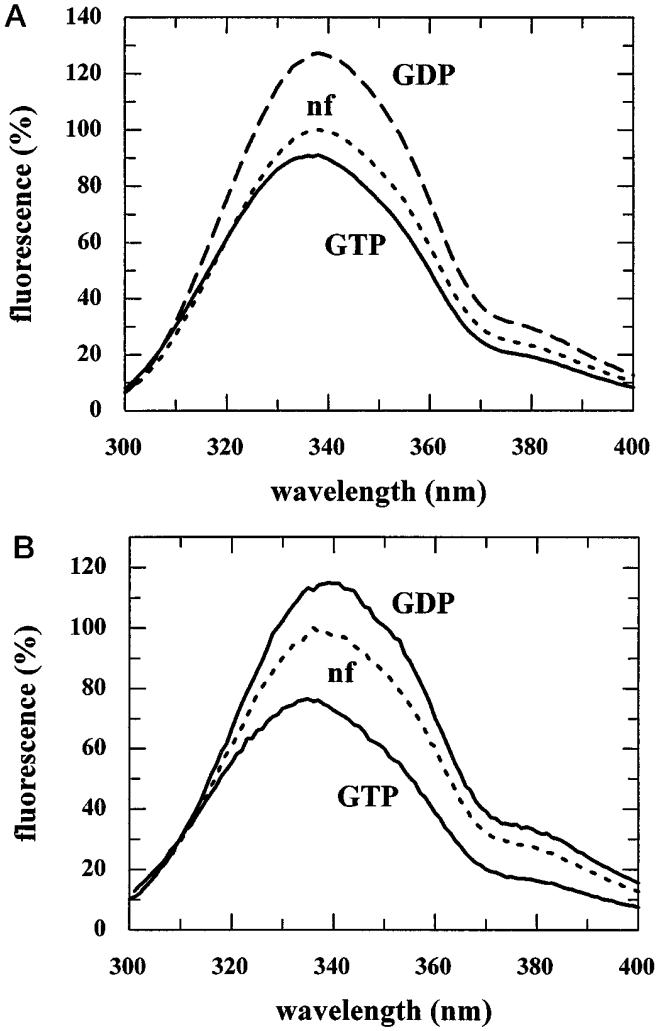

FIG. 1. **Tryptophan emission spectra of 5 μM Rab7 (*A*) and 5 μM Rab5 (*B*) in the nucleotide-free state (*nf*) and after addition of 7 μM GTP or GDP.** Spectra were measured at 25 °C in 40 mM Hepes buffer (pH 7.5) with 10 mM $MgCl_2$ and 2 mM dithioerythritol. Excitation was at 290 nm.

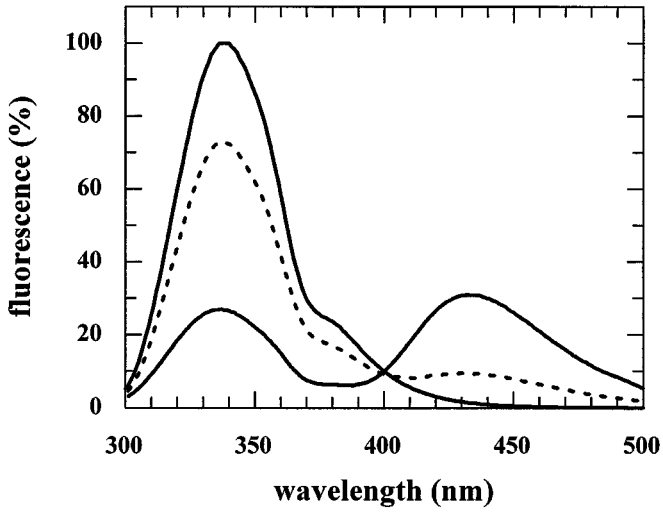

FIG. 2. **Fluorescence energy transfer between tryptophan residues of Rab7 and mantGDP.** The *upper solid curve* shows the emission spectrum of 5 μM Rab7·GDP, the *dashed curve* immediately after addition of 50 μM mantGDP, and the *lower solid curve* after equilibration (*i.e.* after formation of Rab7·mantGDP). Conditions are the same as in Fig. 1.

and 18.3 Å (residues 62, 102, and 142, respectively, in Rab7) from the γ-phosphate of GppNHp in its complex with Rab7[3] and offer a potential signal for observing the interaction of the proteins with substrates and effectors. As shown in Fig. 1, *A* and *B*, the fluorescence emission spectra of nucleotide-free Rab5 and Rab7 are changed significantly on interaction with GTP or GDP. For both proteins, there is an increase in fluorescence yield on interaction with GDP (17% for Rab5 and 28% for Rab7) and a decrease on interaction with GTP (30% for Rab5 and 10% for Rab7). The maximum is shifted from 337 nm in the nucleotide-free proteins and the GTP complex to 340 nm in the GDP complexes. The fluorescence signals were stable for many hours at 25 °C in the GDP state, but begin to decrease noticeably after ~1 h in the nucleotide-free state. As discussed later, the transition from the GTP to the GDP form could be easily followed using the large (~50% in Rab5 and 40% in Rab7) change in fluorescence yields.

Extrinsic Fluorescence—Methylanthraniloyl (mant) derivatives of guanosine nucleotides have been used extensively for studies on GTP-binding proteins (20, 22–27). In general, their fluorescence yield increases significantly on interaction with GTP/GDP binding sites, and this appears to be due at least in part to relief of quenching interactions of the fluorescent moiety with the guanine base, since the mant group on the ribose extends away from the base when guanosine nucleotide derivatives are bound to Ras (28, 29). Binding of mant guanosine nucleotides to the Rab proteins also leads to a substantial increase in fluorescence yield (~100%), so that this can be used as a signal of binding. The presence of tryptophans in the proteins offers the opportunity of observation of fluorescence energy transfer between these residues and the methylanthraniloyl group. As shown in Fig. 2, there is substantial energy transfer in the Rab7·mantGDP complex, as shown by both the decrease in tryptophan fluorescence and the increase in mant fluorescence in comparison with the protein GDP complex and with free mantGDP, respectively (excitation at 290 nm). For Rab5, the quenching of tryptophan fluorescence by mantGDP at the active site is even more pronounced than for Rab7 (data not shown), suggesting that the energy transfer is mainly from residues 62 and 102 in the Rab7 structure and not from Trp142, which has no equivalent in Rab5.

Nucleotide Association (GDP and GTP)—The nucleotide-free proteins were used to investigate the kinetics of nucleotide association. A typical stopped-flow trace is shown for the association of GDP to Rab7 using intrinsic fluorescence as a signal (Fig. 3). The curve could be fitted by a single exponential term, and increasing the concentration of GDP led, initially, to an approximately linear increase in the pseudo-first order rate constant. At higher concentrations, the rates departed from linearity and the data could be fitted by a hyperbolic curve (Fig. 4*A*). This behavior is typical of a two-step binding mechanism in which initial binding is weak and rapid, and this is followed by a second step occurring at a relatively slow rate in which the fluorescence change occurs. The equation relating the pseudo-first order rate constant to the GDP concentration (assuming an excess of GDP over protein) is

$$k_{obs} = \frac{k_{+2}}{1+1/K_1(\mathrm{GDP})} + k_{-2} \qquad \text{(Eq. 1)}$$

for the following scheme.

$$\mathrm{Rab{+}GDP} \underset{}{\overset{K_1}{\leftrightarrows}} \mathrm{Rab{\cdot}GDP} \overset{K_2}{\leftrightarrows} \mathrm{Rab{\cdot}{*}GDP}$$

SCHEME 1

[3] P. Metcalf, personal communication.

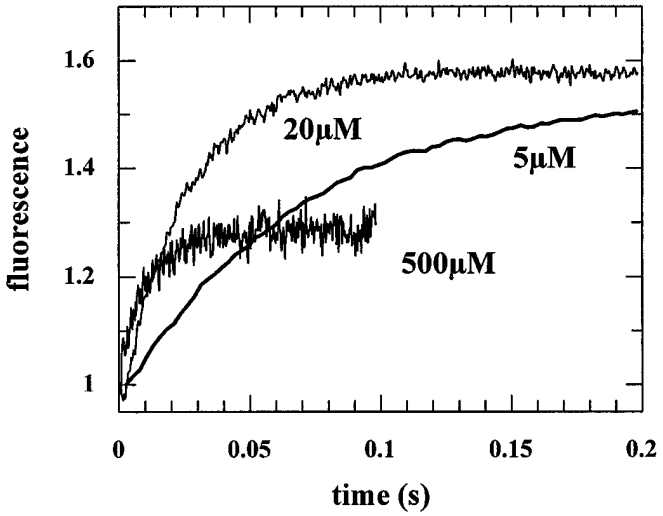

FIG. 3. **Association kinetics of nucleotide-free Rab7 (0.5 μM) and different concentrations of GDP at 20 °C.** Formation of the complex was monitored by tryptophan fluorescence (excitation at 297 nm, detection via a cut-off filter at 320 nm) in a stopped-flow machine. Buffer conditions are the same as in Fig. 1.

Since the hyperbolic fit passes through the origin of the graph in Fig. 4*A*, this means that k_{-2} is very small compared with the smallest observed rate constant measured, so that the second step can be regarded as pseudo-irreversible for the present analysis. The maximum rate reached at high GDP concentration gives a value for k_{+2}, which is 80 s^{-1} in this case. This can be compared with a value of ~20 s^{-1} for Ha-Ras p21 based on a similar analysis (20, 27).

The other constant, which can be extracted from the data, is K_1, the affinity constant for GDP in the first step. This is found to be 4.2×10^4 M^{-1}. The effective second order rate constant for GDP binding at nonsaturating GDP concentrations ($K_1 \times k_{+2}$) is 3.35×10^6 M^{-1} s^{-1}, which is similar to the value for Ha-Ras p21.

A similar analysis could be made of the association kinetics of GTP to Rab7. The results are shown in Fig. 4*B*, and it can be seen that in this case the limiting rate, defining k_{+2}, is, at 32 s^{-1}, significantly slower than for GDP. However, the affinity in the first association step (K_1) is considerably higher than for GDP, so that the effective second order rate constant is higher than that for GDP (Table I).

Similar experiments were performed with nucleotide-free Rab5, and these also led to a hyperbolic dependence of rate against nucleotide (GTP or GDP) concentration. As can be seen from Table II, k_{+2} is similar for GTP and GDP in this case. The K_1 values are also similar for the two nucleotides, but the values are significantly lower than for Rab7, so that the overall effective second order association rate constant is more than an order of magnitude lower than for Rab7.

The analysis of the dependence of the observed rate constant for GDP or GTP binding to Rab5 and Rab7 presented here leads to the conclusion that the binding kinetics can be explained by a two-step mechanism. However, the overall amplitude of the fluorescence change for GDP binding to Rab7 was considerably higher (~60%) than that seen in equilibrium experiments as shown in Fig. 1*A* (28% increase). While it is difficult to compare amplitudes in the stopped-flow and static spectrophotometers accurately because of different optical arrangements and efficiencies, it is highly unlikely that this difference of a factor of 2 is due to differences in machine performance. We checked whether the different excitation wavelengths used (290 nm for the static measurements, 296 nm for the dynamic measurements to reduce attenuation of the signal due to nucleotide

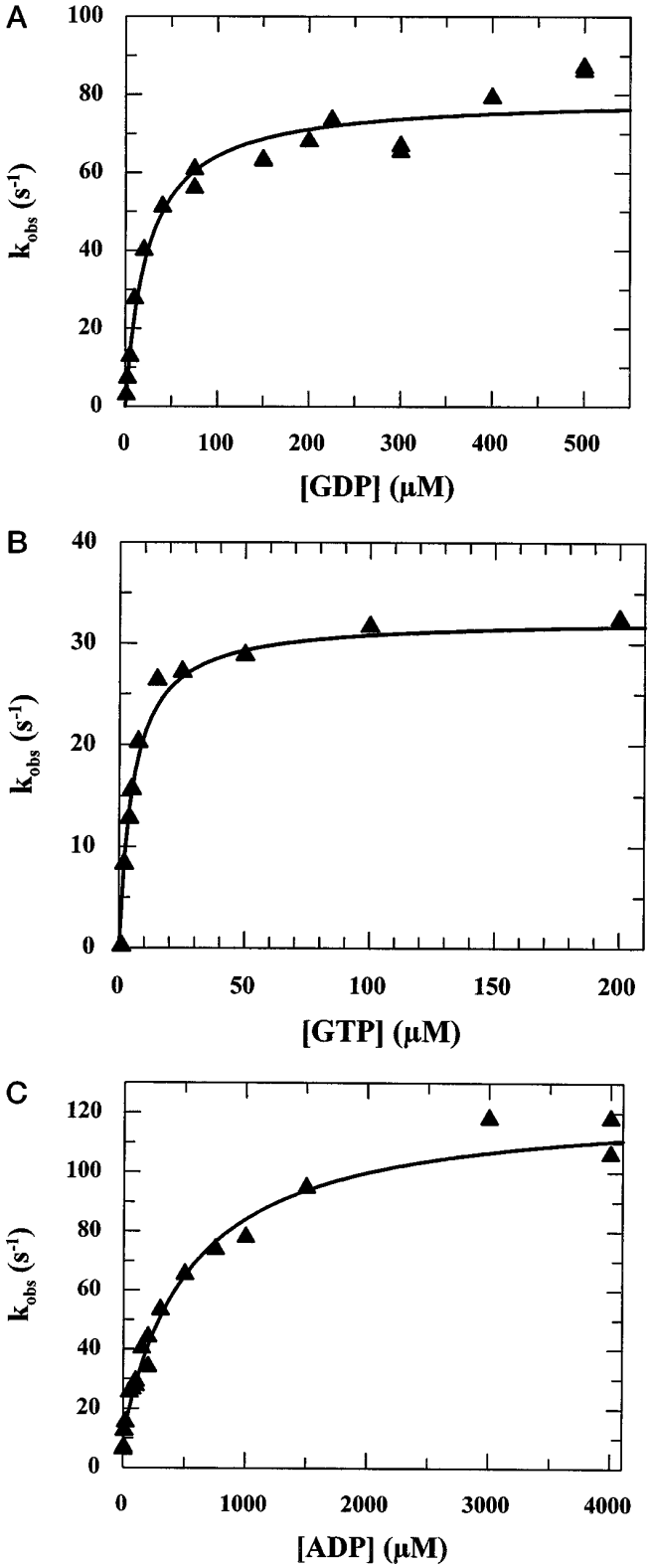

FIG. 4. **Dependence of the pseudo-first order rate constant of association of GDP (*A*), GTP (*B*), and ADP (*C*) with nucleotide-free Rab7 on the concentrations of the respective nucleotide.** Conditions are the same as in Fig. 3.

absorption at high GDP concentrations) was of importance, but obtained identical amplitudes for the GDP-induced change at both wavelengths. We therefore conclude that there is probably a fluorescence change associated with the first binding step in the opposite direction (*i.e.* negative) to that in the second step,

TABLE I
Association and dissociation kinetics of Rab7 and nucleoside di- and triphosphates at 20 °C
k_{on} refers to the product of K_1 and k_{+2} and is the effective second order rate constant of binding at low (*i.e.* $\ll 1/K_1$) nucleotide concentrations.

Nucleotide	Association, K_1	k_{+2}	k_{on}	Dissociation, k_{on}	Affinity, $K_a\times$
	$\times 10^{-4}$ M^{-1}	s^{-1}	$\times 10^{-6}$ M^{-1} s^{-1}	$\times 10^{5}$ s^{-1}	$\times 10^{-10}$ M^{-1}
GDP	4.2	80	3.35	0.8	42
GTP	18.3	32	5.95	1	60
XDP	4	45.7	1.83	320	0.057
ADP	0.18	113	0.21	1,070,000	0.000002
ATP	0.85	24.3	0.21	800,000	0.000003

and that the large amplitude seen in the stopped-flow experiments is the net result of an initial drop in fluorescence within the dead time of the apparatus followed by an observable increase to the final level characteristic of the Rab7 GDP complex.

Nucleotide Dissociation (GDP and GTP)—The measurement of the dissociation rate constants of mantGDP from its complex with GTP-binding proteins can be conveniently measured by displacing the bound fluorescent nucleotide with a large excess of unlabeled nucleotide. The rate constant for release of the natural nucleotides is more difficult to measure spectroscopically, since addition of a large excess of mantGDP or mantGTP to a protein-GDP or -GTP complex produces a large background fluorescence if the mant group is excited directly at 350–370 nm. This problem is reduced significantly by using the energy transfer effect described in a previous section. Thus, a ~20–50-fold excess of mantGDP can be added to a Rab. GDP complex, and on exciting at 290 nm with measurement of the fluorescence intensity at 440 nm, the increase in intensity can be used to monitor replacement of GDP by mantGDP, which is limited by the rate of GDP release under these conditions. The rate constant of GDP release from Rab7 was found to be 8×10^{-6} s^{-1} at 20 °C, and 3.9×10^{-5} s^{-1} at 37 °C (Rab5: 10^{-5} s^{-1} at 20 °C, 4.3×10^{-5} s^{-1} at 37 °C). These values are considerably lower than the rate constant of GDP dissociation from Ha-Ras p21 and explain the greater difficulty of preparation of the Rab proteins in the nucleotide-free state.

Measurement of the dissociation rate of GTP is more complicated, since hydrolysis and dissociation take place on the same time scale. The approach adopted to determine the GTP dissociation rate is that of measurement of the hydrolysis rate and extent of already bound GTP in the presence of excess GDP. Under these conditions, a fraction of the bound GTP is hydrolyzed to GDP, and a fraction dissociates as GTP, after which it is prevented from rebinding by the excess GDP free in solution. It can be shown that the time dependence of GTP hydrolysis is given as follows.

$$[\mathrm{GTP}]_t = [\mathrm{GTP}]_o\left[1 - \frac{k_{\mathrm{cat}}}{k_d + k_{\mathrm{cat}}}(1 - e^{-(k_d + k_{\mathrm{cat}})t})\right] \qquad \text{(Eq. 2)}$$

Fig. 5 shows the GTP hydrolysis kinetics of Rab7 in the absence and presence of a 50-fold excess of GDP. It can be seen that there is a noticeable effect of GDP on the hydrolysis kinetics, and in particular, a significant amount of residual unhydrolyzed GTP remains at times when GTP hydrolysis is complete in the absence of GDP. In principle, there is information on the rate constants for GTP hydrolysis and dissociation in the observed rate constant for the reaction, which is the sum of the independently measured cleavage rate constant and the dissociation rate constant, and also in the plateau level of GTP when the reaction is essentially finished. The best estimate of the rate constant can be obtained by fitting to the complete Equation 2, and this led to a value of 2.7×10^{-5} s^{-1} at 37 °C for k_d (k_{-2} in Scheme 1) and 7.95×10^{-5} s^{-1} for k_{cat}, which agrees well with the independently measured value of 9×10^{-5} s^{-1} (see below). The dissociation rate constants for GTPγS were

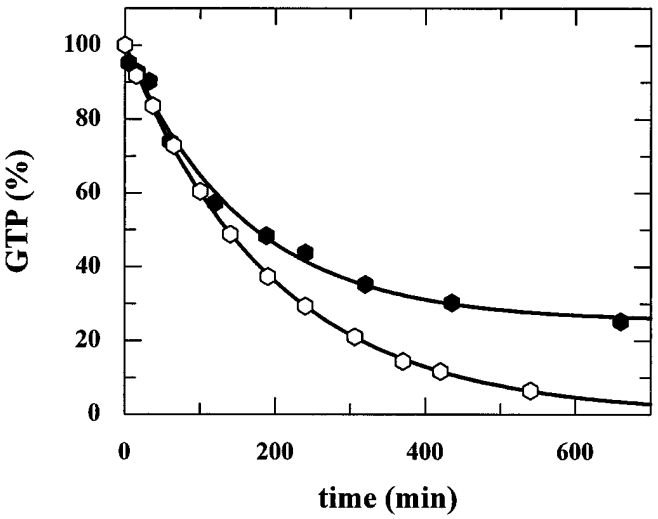

FIG. 5. **Hydrolysis of GTP by Rab7.** Empty symbols show the time course of GTP hydrolysis of a stoichiometric complex of Rab7 and GTP at 37 °C (150 μM in 40 mM Hepes buffer at pH 7.5). *Filled symbols* show the time course when GDP (7 mM) was added 5 s after starting the hydrolysis reaction by addition of 10 mM $MgCl_2$. The reaction was followed by determining the concentrations of GTP and GDP by HPLC. See "Materials and Methods" for a description of the procedure used.

determined using similar methods. For Rab7, it was almost identical to the rate of dissociation of GTP (at 37 °C, the rate of GTP dissociation was 3×10^{-5} s^{-1}, that of GTP(γS) 3.6×10^{-5} s^{-1}).

The dissociation rate constant of GTP from its complex with Rab5 could not be measured by this method because of the much higher rate of GTP hydrolysis in comparison with the slow off-rate of GTP, so that there was no detectable difference in the rate or extent of GTP hydrolysis in the presence or absence of excess GDP. This question might be answered using a more sensitive technique in which radioactively labeled GTP of high specific activity is used to allow detection of a small residual amount of substrate. Since the rates of GTP and GTPγS from their complexes with Rab7 were almost identical, we assume that this also applies to Rab5 and have therefore included the (measurable) value for GTPγS dissocation in Table II.

The affinity of the Rab proteins for GTP and GDP can be calculated from the kinetic constants for the association and dissociation reactions (Tables I and II). Like the other small GTP-binding proteins already investigated in detail (Ras, Ran), the overall affinity of Rab5 and Rab7 for guanosine nucleotides is very high (of the order of 10^{11} M^{-1}). Previously reported values of binding constants for the related Sec4 protein were determined using a direct titration method, which does not take acount of the bound nucleotide present in all preparations of GTP-binding proteins (30). As pointed out (21), this cannot give proper estimates of affinities, and the value obtained is dependent on the absolute concentration of protein used in the determination. There is significant variation in the rate and equilibrium constants for the individual steps in the binding

TABLE II
Association and dissociation kinetics of Rab5 and nucleoside di- and triphosphates at 20 °C

Nucleotide	Association, K_1	k_{+2}	k_{on}	Dissociation, k_{on}	Affinity, K_a
	$\times 10^{-4}$ M^{-1}	s^{-1}	$\times 10^{-6}$ M^{-1}	$\times 10^{5}$ s^{-1}	$\times 10^{-10}$ M^{-1}
GDP	0.74	28	0.21	0.6	3.5
GTP	0.86	32	0.28	0.8 (GTPγS)	3.5
XDP	0.177	28	0.05	600	0.0008
ADP	0.18	20	0.036	900,000	0.0000004
ATP	0.47	5.5	0.026	250,000	0.000001

mechanism. Ras (20) and Rab7 (this work) show similar values of $\sim 10^5$ M^{-1} for the initial binding, whereas it is weaker in Rab5 (less than 10^4 M^{-1}) and even more so in EF-Tu ($\sim 10^3$ M^{-1}). The forward rate constant for the second step varies from ~ 20 s^{-1} for Ras to several hundred s^{-1} (depending on the nucleotide) for EF-Tu (31). The most significant difference is, however, in the reverse rate constant for the second step, which ranges from $\sim 10^{-5}$ s^{-1} for the Rab proteins (for GTP and GDP) to $\sim 10^{-2}$ s^{-1} for GTP from EF-Tu (10^{-3} s^{-1} for GDP). This large difference in the value of k_{-2} is the main reason for the lower affinity of EF-Tu for nucleotides, particularly for GTP, when compared with the proteins of the Ras family proteins.

The two Rab proteins investigated here show very low rates of spontaneous GDP release, suggesting that replacement of GDP by GTP occurs in a tightly regulated manner. This is a property shared with trimeric G-proteins, for which it appears to be difficult to even determine the spontaneous rate of release, and other proteins of the Ras superfamily. Receptor-mediated release of GDP from the α-subunits of G-proteins is a well known phenomenon, as is the catalysis of GTP/GDP exchange for ribosomal factors, and nucleotide release factors have been identified for a number of small GTP-binding proteins. The most detailed characterization of the kinetics of such an exchange reaction has been presented for the nuclear Ras-related protein Ran and its exchange factor RCC1 (32). In the latter case, acceleration of GDP release in the ternary complex between the GTPase, GDP, and the exchange factor is of the order of a factor of 10^6. In the case of the Rab proteins and their homologs, several examples of exchange factors have identified (7, 8, 33), although the point at which they act in the reaction cycle is not clear. The exchange factors appear to be specific with respect to the particular Rab protein. In contrast, factors which inhibit the release of GDP (GDIs), although existing as several isoforms, are apparently able to interact with many or all Rabs. Their role appears to be to interact with prenylated Rab proteins in the GDP form to produce a complex that is soluble and from which GDP dissociation is even slower than in the absence of the GDI. Thus, regulation is made even more stringent in this stage of the cycle. In summary, it seems highly likely that regulation of GDP release from Rab proteins is highly regulated, and in agreement with this, it has been shown that membrane association of Rab5 (5) and Rab9 (6) is accompanied by GDP/GTP exchange.

Interaction of Rab Proteins with XTP and ATP—GTP-binding proteins are highly specific for guanosine nucleotides. A recent study showed that Ha-Ras p21 discriminates against ITP and XTP by a factor of 100-1000 and against ATP by a factor of more than 10^6 (26). The mechanism of this discrimination arises partly from loss of hydrogen binding interactions on changing the structure of the base and in the case of ATP also from steric hindrance between the 6-amino group and the protein backbone (26). In the present work, XDP, ADP, and ATP were examined as ligands for Rab5 and Rab7. As for the guanosine nucleotides, protein fluorescence provides a convenient manner of observing these interactions directly. As can be seen from the values given in Tables I and II, XDP shows similar binding characteristics to GDP, with the exception that the dissociation rate constant (k_{-2}) is increased by factors of ~300 and 600 for Rab7 and Rab5, respectively. Together with a reduction in the effective on-rate, particularly for Rab5, this results in a lowering of affinity by a factor of ~1000 in comparison with GDP, in agreement with the data obtained for Ha-Ras p21 (26).

Measurement of the affinity of ADP or ATP to GTP-binding proteins can only be achieved by transient kinetic methods, since the more classical procedure of measuring the affinity by inhibition of GDP binding cannot be used because of the prohibitively high concentrations of adenosine nucleotide which would be needed (26). For Ha-Ras p21, a relatively indirect method was used (analysis of the effect of ATP on the association kinetics of mantGDP) for which a numerical integration and fitting procedure was needed to extract the rate constants for ATP binding and dissociation. In contrast, the tryptophan signal from the Rab proteins could be used directly to monitor ADP or ATP binding. The results for ADP are shown in Fig. 4*C*, and it can be seen that as for the guanosine and xanthosine nucleotides, there is a hyperbolic dependence of the observed first order rate constant on the ADP concentration. Surprisingly, the value of k_{+2} is higher then for GDP (113, *cf.* 80 s^{-1}), but the fitted curve showed two major differences. First, the intercept on the *y* axis is not immeasurably small, but has a well defined value of 10.7 s^{-1}, and this corresponds to the value for k_{-2}. This is a factor of 10^6 greater than for GDP. The value for Ha-Ras p21 and ADP is 2.1 s^{-1}. Taken together with the respective forward rate constants, the equilibrium constant for the second step with ATP or ADP is of the order of 10 for Rab7, Rab5, and Ha-Ras p21, compared with 10^5-10^6 for the guanosine nucleotides. Second, the value for K_1 is considerably lower for ATP or ADP than for the guanosine nucleotides. The combination of both effects leads to an overall difference in affinity of $\sim 10^7$ between guanosine and adenosine nucleotides, for both the Rab and Ras proteins. We have shown recently that an almost identical degree of discrimination is shown by EF-Tu (31). The result is of particular interest for Rab5, since it was reported previously that this protein binds ATP with similar affinity to GTP (34). The results presented here demonstrate that this is clearly not the case and that discrimination against ATP and ADP is as dramatic as for Ha-Ras p21, EF-Tu, and Rab7 proteins.

Interaction of Mg^{2+} with Rab-Nucleotide Complexes—In common with other nucleoside triphosphatases and kinases, Mg^{2+} is an essential cofactor for the GTP-binding proteins. A detailed study of the interaction of Mg^{2+} with Ha-Ras p21 has been published, and for this purpose kinetic methods, NMR and nucleotide (extrinsic) fluorescence were used (22). In the present work it was found that significant changes in protein fluorescence occur on interaction of Mg^{2+} with Rab7. Fig. 6 shows the results of removal from and readdition of Mg^{2+} to Rab7·GDP, using tryptophan fluorescence as a monitor of the interaction. It can be seen that dissociation of Mg^{2+} leads to a decrease in fluorescence intensity of ~20%, which can be reversed by addition of excess Mg^{2+}. The rate of Mg^{2+} dissociation is too fast to measure in a standard fluorescence spectrophotometer, but can be followed conveniently in the stopped-

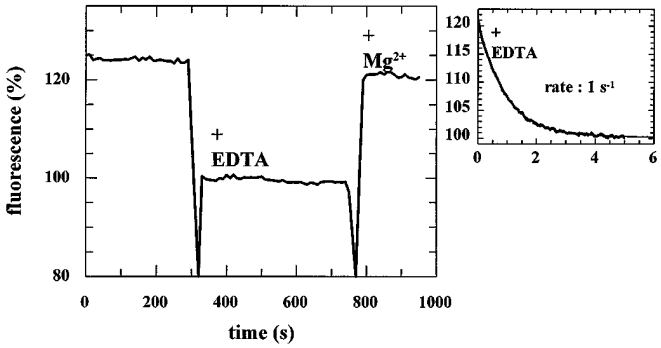

FIG. 6. **Interaction of Mg^{2+} with Rab7·GDP.** The EDTA-induced dissociation of Mg^{2+} from 5 μM Rab7·GDP at 25 °C led to a rapid decrease in intrinsic fluorescence, which was too fast to measure in the fluorescence spectrophotomer. Readdition of Mg^{2+} in excess of EDTA led to a rapid return to the starting fluorescence level. The *inset* shows the first phase (removal of Mg^{2+}) at higher time resolution, as measured in the stopped flow machine.

flow machine, which leads to the data shown in Fig. 6, which can be fitted by an exponential term with a rate constant of 1.0 s^{-1}. By contrast, removal of Mg^{2+} from Rab7·GTP leads to an increase of fluorescence of ~10% at a much slower rate (8×10^{-3} s^{-1}) than from Rab7·GDP (data not shown). The measured rate constants were independent of the EDTA concentration. These changes could also be used to measure the kinetics of Mg^{2+} binding to Rab7·GDP and Rab7·GTP, respectively. Both showed a linear dependence of the pseudo-first order rate constant on the magnesium concentration. The second order rate constant for association with Rab7·GDP was 1.8×10^5 M^{-1} s^{-1}, for Rab7·GTP 2.8×10^6 M^{-1} s^{-1}. Taken together with the dissociation rate constants, the Mg^{2+} dissociation constants can be calculated to be 5.5 μM and 2.8 nM for the Rab7·GDP and Rab7·GTP complexes, respectively. The corresponding values for Ras are 2.8 μM and 22 nM (22). It is of interest to note that the effective second order rate constants reported here are significantly lower than those reported for the interaction of Mg^{2+} with the deprotonated forms of ADP and ATP (3×10^6 M^{-1} s^{-1} and 1.2×10^7 M^{-1} s^{-1}, respectively; Ref. 35). This may arise from the fact that there is a certain degree of charge neutralization in the complexes of the nucleotides with the protein, thus reducing electrostatic interactions which may facilitate formation of the initial collision complexes. In contrast, the dissociation rates from the Rab7·GDP and Rab7·GTP complexes (see above) are reduced dramatically in comparison with the corresponding rates from the free metal-nucleotide complexes (2500 and 1200 s^{-1} for ADP and ATP, respectively; Ref. 35). This is presumably due to additional interactions of the metal ion with the protein molecule, both direct and via water molecules.

The dramatic increase in affinity for Mg^{2+} in the GTP complex when compared with the GDP complex appears to be the result of the additional interaction of the metal ion with the γ-phosphate group. In the structure of the GTP-bound state of the Ras protein, it can be seen that there are two direct interactions of the metal ion with the protein (side chain hydroxyls of Ser-17 and Thr-35) and one interaction with the γ-phosphate group. In the GDP state, there is only one phosphate interaction (β-phosphate group), and the interaction with Thr-35 is lost. The remaining two (GTP) or four (GDP) ligands of the hexacoordinated ion are water molecules. In the case of Rab7, there appear to be analogous interactions with the protein and the nucleotide (Thr-22 and Thr-40).[3]

As for other GTP-binding proteins, removal of the Mg^{2+} ions leads to a significant increase in the dissociation rate of the bound nucleotide (from 8×10^{-6} s^{-1} to 2.1×10^{-3} s^{-1} for GDP and from 1.3×10^{-5} s^{-1} to 4.7×10^{-3} s^{-1} for GTP). This was

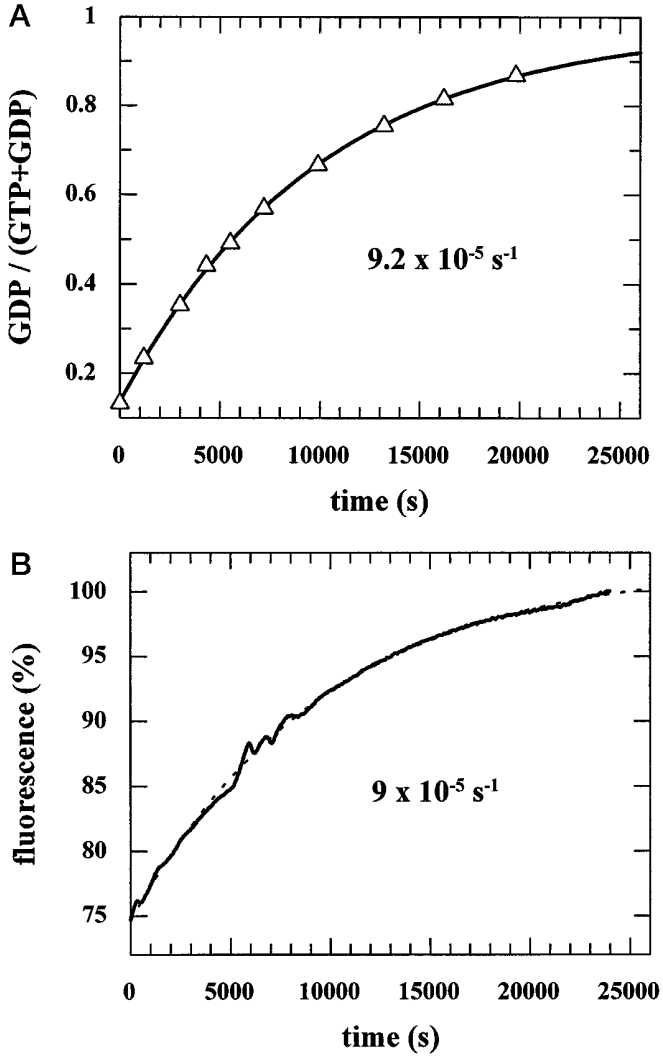

FIG. 7. **Single turnover of GTP by Rab7 (5 μM) at 37 °C.** *A* shows the time dependence of the relationship of GDP to total nucleotide as function of time (determined by HPLC analysis), while *B* shows the time dependence of the increase in fluorescence.

monitored by displacing GDP or GTP with excess mantGDP using fluorescence energy transfer as a signal for dissociation.

GTP Hydrolysis by Rab Proteins—The large difference in the fluorescence yield of the two Rab proteins in the presence of GDP or GTP results in an easily monitored signal for GTP hydrolysis. As shown in Fig. 7, *A* and *B*, the rate constant for the fluorescence change seen after triggering GTP hydrolysis in the Rab7·GTP complex is identical to that obtained for the conversion of GTP to GDP in this complex as measured by HPLC analysis of the nucleotide content. The rate constant of 9×10^{-5} s^{-1} is significantly slower than that for the Ras protein under the same conditions (4×10^{-4} s^{-1}; Ref. 26). In contrast, Rab5 hydrolyzes GTP at a significantly faster rate (see Table III). It is of interest to note that the GTP hydrolysis rates of the structurally highly related small GTP-binding proteins vary over more than an order of magnitude, even though groups identified as being important for the hydrolysis mechanism are conserved.

Similar behavior of the tryptophan fluorescence of the small GTP-binding protein Cdc42Hs, a member of the Rho subgroup of the Ras superfamily, was seen on GTP hydrolysis, in this case resulting in a 30% increase of fluorescence intensity (36). The rate constant for GTP hydrolysis in this case is 1.3–1.8 $\times$ 10^{-3} s^{-1}.

TABLE III
Rate constants for GTP (or GTPγS) cleavage by Rab7 and Rab5 at different temperatures

Temperature	Rab7	Rab5
5 °C	2.6×10^{-6} s^{-1}	1.8×10^{-4} s^{-1}
25 °C	4.5×10^{-5} s^{-1}	5.5×10^{-4} s^{-1}
37 °C	0.9×10^{-4} s^{-1}	2×10^{-3} s^{-1}
37 °C, GTPγS	2.5×10^{-5} s^{-1}	3.7×10^{-5} s^{-1}

The variation of GTPase rate in these closely related proteins is of interest with respect to their cell biological role. While it is clear that additional factors are involved in accelerating the slow basal rate of many of these proteins (GAPs and perhaps, in some cases, interaction with molecules which act as effectors, or transmitters, of their action), it is possible that the intrinsic rate is high enough in some cases to allow the biological role to be fulfilled without acceleration by other components or interactions. In the case of Rab5, the half-life for GTP hydrolysis at 37 °C is only 6 min. Transport from the plasma membrane to the early endosome takes about 2 min, while endosome fusion takes about 10 min (37, 38). Concerning Rab7, the transport from the early to the late endosomes takes 30–60 min, which is not too far removed from the rate of GTP hydrolysis by Rab7 reported here ($t_{½}$ = 120 min; Ref. 39). Transport from the late endosomes to the trans-Golgi network takes ~3 h (40), while the $t_{½}$ for GTP hydrolysis by the involved Rab9 is 140 min. Thus, although the activity of GAPs or interactions with target molecules that may accelerate the intrinsic GTPase rates is likely to be of importance for the action of some Rab proteins, it is not clear that this applies generally.

The mechanistic implications of the variation in rates is also of interest. The high sequence and structural homology, particularly around the active site, is an aspect which must be accounted for in the current discussion of GTPase mechanisms by GTP-binding proteins (41–45). The contrast between Rab5 and Rab7 is particularly striking, in view of their similarity in other respects. The variation in GTPase rate must be explained in view of the fact that all residues so far implicated in the hydrolysis mechanism are identical in the two proteins. This suggests that minor changes in the local structure of the active site (and perhaps corresponding changes in the electrostatic environment of the γ-phosphate and attacking water molecule) can have a pronounced effect on the hydrolysis reaction.

Fluorescence Quenching Experiments—These experiments were performed with two different quenchers, acrylamide and iodide. Whereas acrylamide is a relatively good quencher, indicating that the tryptophans residues are not buried in the protein, quenching by iodide is very weak, suggesting that the tryptophan residues are in an electrostatically negative environment. Interestingly, there was a significant difference in quenching by acrylamide in the Rab7·GDP and Rab7·GTP complexes. The results (Fig. 8) are plotted according to the Stern-Vollmer equation (46).

$$F_0/F = 1 + K_{sv}[Q] \quad \text{(Eq. 3)}$$

where F_0 is the fluorescence intensity in the absence of quencher, F the fluorescence in its presence, Q the concentration of quencher, and K_{sv} the Stern-Vollmer constant. The large difference in K_{sv} for acrylamide quenching for the Rab7·GDP and Rab7·GTP complexes suggests that a substantial change in the environment of the tryptophan residues occurs on GTP hydrolysis, confirming the impression gained from the comparison of fluorescence yields (Fig. 7*B*). In both respects, *i.e.* quantum yield and quenching efficiency of acrylamide, the nucleotide free protein is intermediate in behavior between the GTP and GDP forms, suggesting distinct conformations of the three states. As is known from detailed studies of the Ras protein, these changes are mainly in the loop 2, loop 4, and possibly α-helix 2 region of the structure, and the biological significance is that the interaction of the protein with its partner proteins GAP and Raf kinase are different in the two forms.

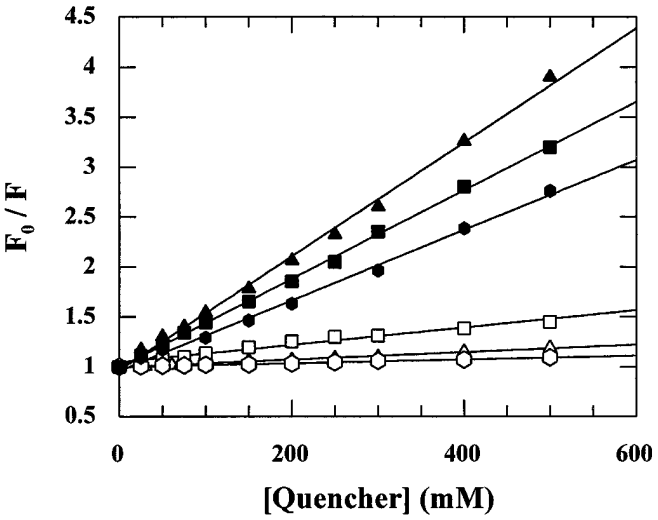

FIG. 8. **Stern-Volmer plots of acrylamide (*solid symbols*) and iodide (*empty symbols*) quenching of tryptophan fluorescence of Rab7 (1 μM) in the nucleotide-free state (*square symbols*), the GDP bound state (*triangles*), or the GTP state (*hexagons*) at 25 °C.**

CONCLUSION

The results reported here confirm a high degree of mechanistic similarity between the GTP-binding proteins. This includes very high affinity for GTP and GDP, with corresponding extremely slow rates of spontaneous dissociation. This implies tight regulation of this event in the cycles regulated by Rab proteins. As for Ras and EF-Tu, two-step association kinetics are observed for nucleotides, and there is pronounced nucleotide specificity for the binding reaction. Thus, the previously reported dramatic discrimination of Ras against ATP (26) is reproduced quantitatively to the same extent by EF-Tu (31) and now Rab5 and Rab7 (this work). This was somewhat surprising, since it had been reported previously that ATP binds with much higher relative affinity to Rab5 than to Rab7 and other GTP-binding proteins (34). The results presented here leave no doubt about the fact that discrimination against ATP is quantitatively almost identical for the GTP-binding proteins and that the mechanism of this discrimination is the same as that demonstrated for Ras (26).

In future work on the Rab proteins, the methods developed here will be applied to their prenylated forms and will include detailed investigations of their interaction with partner molecules.

Acknowledgment—We thank Andrea Beste for technical support and Peter Metcalf (EMBL, Heidelberg, Germany) for sharing information on the three-dimensional structure of Rab7 before publication. We also thank Angela Wandinger-Ness (Northwestern University, Evanston, IL) for recloning the coding regions for Rab5 and Rab7 into the pET constructs.

REFERENCES

1. Novick, P., and Brennwald, P. (1993) *Cell* **75,** 597–601
2. Nuoffer, C., and Balch, W. E. (1994) *Annu. Rev. Biochem.* **63,** 949–990
3. Zerial, M., and Stenmark, H. (1993) *Curr. Biol.* **5,** 613–620
4. Pfeffer, S. R. (1994) *Curr. Biol.* **6,** 522–526
5. Ullrich, O., Horiuchi, H., Bucci, C., and Zerial, M. (1994) *Nature* **368,** 157–160
6. Soldati, T., Shapiro, A. D., Dirac-Svejstrup, A. B., and Pfeffer, S. R. (1994) *Nature* **369,** 76–78
7. Moya, M., Roberts, D., and Novick, P. (1993) *Nature* **361,** 460–463
8. Burton, J., Roberts, D., Montaldi, M., Novick, P., and De Camilli, P. (1993)

Nature **361,** 464–467
9. Burstein, E. S., Linko-Stentz, K., Lu, Z., and Macara, I. G. (1991) *J. Biol. Chem.* **266,** 2689–2692
10. Strom, M., Vollmer, P., Tan, T. J., and Gallwitz, D. (1993) *Nature* **361,** 736–739
11. Pfeffer, S. R., Dirac-Svejstrup, A. B., and Soldati, T. (1995) *J. Biol. Chem.* **270,** 17057–17059
12. Andres, D. A., Seabra, M. C., Brown, M. S., Armstrong, S. A., Smeland, T. E., Cremers, F. P. M., and Goldstein, J. L. (1993) *Cell* **73,** 1091–1099
13. Shirataki, H., Kaibuchi, K., Sakoda, T., Kishida, S., Yamaguchi, T., Wada, K., Miyazaki, M., and Takai, Y.(1993) *Mol. Cell. Biol.* **13,** 2061–2068
14. Li, C., Takei, K., Geppert, M., Daniell, L., Stenius, K., Chapman, E. R., Jahn, R., De Camilli, P., and Südhof, T. C. (1993) *Neuron* **13,** 885–898
15. Stenmark, H., Vitale, G., Ullrich, O., and Zerial, M. (1995) *Cell* **83,** 423–432
16. Chavrier, P., Vingron, M., Sander, C., Simons, K., and Zerial, M. (1990) *Mol. Cell. Biol.* **10,** 6578–6585
17. Studier, W., Rosenberg, A. H., Dunn, J. J., and Dubendorf, J. W. (1990) *Methods Enzymol.* **185,** 60–89
18. Tucker, J., Sczakiel, G., Feuerstein, J., John, J., Goody, R. S., and Wittinghofer, A. (1986) *EMBO J.* **5,** 1351–1358
19. Steele-Mortimer, O., Clague, M. J., Huber, L. A., Chavrier, P., and Gorvel, J.-P. (1994) *EMBO J.* **13,** 34–41
20. John, J., Sohmen, R., Feuerstein, J., Linke, R., Wittinghofer, A., and Goody, R. S. (1990) *Biochemistry* **29,** 6058–6065
21. Goody, R. S., Frech, M., and Wittinghofer, A. (1991) *Trends Biochem. Sci.* **16,** 327–328
22. John, J., Rensland, H., Schlichting, I., Vetter, I., Borasio, G. D., Goody, R. S., and Wittinghofer, A. (1993) *J. Biol. Chem.* **268,** 923–929
23. John, J., Frech, M., Feuerstein, J., Goody, R. S., and Wittinghofer, A. (1989) in *The Guanine-Nucleotide Binding Proteins* (Bosch, L., Kraal, B., and Parmeggiani, A., eds) pp. 209–214, Plenum Publishing Corp., New York
24. Moore, K. J. M., Webb, M. R., and Eccleston, J. F. (1993) *Biochemistry* **32,** 7451–7459
25. Neal, S. E, Eccleston, J. F., and Webb, M. R. (1990) *Proc. Natl. Acad. Sci. U. S. A.* **87,** 3652–3565
26. Rensland, H., Lautwein, A., Wittinghofer, A., and Goody, R. S. (1991) *Biochemistry* **30,** 11181–11185
27. Rensland, H., John, J., Linke, R., Simon, I., Schlichting, I., Wittinghofer, A., and Goody, R. S. (1995) *Biochemistry* **34,** 593–599
28. Goody, R. S., Pai, E. F., Schlichting, I., Rensland, H., Scheidig, A., Franken, S., and Wittinghofer, A. (1992) *Philos. Trans. R. Soc. Lond. B* **336,** 3–11
29. Scheidig, A., Sanchez-Llorente, A., Lautwein, A., Pai, E. F., Corrie, J. E. T., Reid, G., Wittinghofer, A., and Goody, R. S. (1994) *Acta Crystallogr.* **D50,** 512–520
30. Kabcenell, A. K., Goud, B., Northup, J. K., and Novick, P. J. (1990) *J. Biol. Chem.* **265,** 9366–9372
31. Wagner, A., Simon, I., Sprinzl, M., and Goody, R. S. (1995) *Biochemistry* **34,** 12535–12542
32. Klebe, C., Prinz, H., Wittinghofer, A., and Goody, R. S. (1995) *Biochemistry* **34,** 12543–12552
33. Burstein, E. S., and Macara, I. G. (1992) *Proc. Natl. Acad. Sci. U. S. A.* **89,** 1154–1158
34. Zahraoui, A., Touchot, N., Chardin, P., and Tavitian, A. (1989) *J. Biol. Chem.* **264,** 12394–12401
35. Eigen, M., and Hammes, G. G. (1960) *J. Am. Chem. Soc.* **82,** 5951–5952
36. Leonard, D. A., Evans, T., Hart, M., Cerione, R. A., and Manor, D. (1994) *Biochemistry* **33,** 12323–12328
37. Griffiths, G., Back, R., and Marsh, M. (1989) *J. Cell Biol.* **109,** 2703–2720
38. Gruenberg, J., and Maxfield, F. R. (1995) *Curr. Opin. Cell Biol.* **7,** 552–563
39. Feng, Y., Press, B., and Wandinger-Ness, A. (1995) *J. Cell Biol.* **131,** 1–18
40. Goda, Y., and Pfeffer, S. R. (1988) *Cell* **55,** 309–320
41. Pai, E., Krengel, U., Petsko, G., Goody, R. S., Kabsch, W., and Wittinghofer, A. (1990) *EMBO J.* **9,** 2351–2359
42. Prive, G. G., Milburn, M. V., Tong, L., de Vos, A. M., Yamaizumi, Z., Nishimura, S., and Kim, S. H. (1992) *Proc. Natl. Acad. Sci. U. S. A.* **89,** 3649–3653
43. Sondek, J., Lambright, D. G., Noel, J. P., Hamm, H. E., and Sigler, P. B. (1994) *Nature* **372,** 276–279
44. Goody, R. S. (1994) *Nature* **372,** 220–221
45. Schweins, T., Geyer, M., Scheffzek, K., Warshel, A., Kalbitzer, H. R., and Wittinghofer, A. (1995) *Struct. Biol.* **2,** 36–44
46. Lehrer, S. S. (1971) *Biochemistry* **10,** 3254–3263